



Published in final edited form as:

*Neuroimage*. 2015 June ; 113: 397–406. doi:10.1016/j.neuroimage.2015.02.070.

## Miniaturized Optical Neuroimaging in Unrestrained Animals

Hang Yu<sup>1</sup>, Janaka Senrathna<sup>1</sup>, Betty M. Tyler<sup>2</sup>, Nitish V. Thakor<sup>1</sup>, and Arvind P. Pathak<sup>3</sup>

<sup>1</sup>Department of Biomedical Engineering

<sup>2</sup>Neurosurgery

<sup>3</sup>Russell H. Morgan Department of Radiology and Radiological Science, The Johns Hopkins University School of Medicine, Baltimore, USA

### Abstract

The confluence of technological advances in optics, miniaturized electronic components and the availability of ever increasing and affordable computational power have ushered in a new era in functional neuroimaging. Namely, an era in which neuroimaging of cortical function in unrestrained and unanesthetized rodents has become a reality. Traditional optical neuroimaging required animals to be anesthetized and restrained. This greatly limited the kinds of experiments that could be performed *in vivo*. Now one can assess blood flow and oxygenation changes resulting from functional activity, image functional response in disease models such as stroke and seizure, and even conduct long-term imaging of tumor physiology, all without the confounding effects of anesthetics or animal restraints. These advances are shedding new light on mammalian brain organization and function, and helping to elucidate loss of this organization or ‘dysfunction’ in a wide array of central nervous system disease models.

In this review, we highlight recent advances in the fabrication, characterization and application of miniaturized head-mounted optical neuroimaging systems pioneered by innovative investigators from a wide array of disciplines. We broadly classify these systems into those based on exogenous contrast agents, such as single- and two-photon microscopy systems; and those based on endogenous contrast mechanisms, such as multispectral or laser speckle contrast imaging systems. Finally, we conclude with a discussion of the strengths and weaknesses of these approaches along with a perspective on the future of this exciting new frontier in neuroimaging.

### Keywords

optical; imaging; freely moving; unanesthetized; tetherless; miniaturized

---

**Address for Correspondence:** Dr. Arvind P. Pathak, Division of Cancer Imaging Research, Russell H. Morgan Department of Radiology and Radiological Science, The Johns Hopkins University School of Medicine, 720 Rutland Ave, 217 Traylor Bldg., Baltimore, MD 21205, U. S. A., Tel: (410) 955-4213, Fax: (410) 614-1948, pathak@mri.jhu.edu.

**Publisher's Disclaimer:** This is a PDF file of an unedited manuscript that has been accepted for publication. As a service to our customers we are providing this early version of the manuscript. The manuscript will undergo copyediting, typesetting, and review of the resulting proof before it is published in its final citable form. Please note that during the production process errors may be discovered which could affect the content, and all legal disclaimers that apply to the journal pertain.

## Introduction

Imaging the brain has provided unprecedented insights into its functioning as well as disruption of this function due to various neuropathologies. Noninvasive imaging techniques such as functional Magnetic Resonance Imaging (fMRI) (Heeger et al. 2002), Positron Emission Tomography (PET) (Nasrallah et al. 2013) and Computed Tomography (CT) (Cianfoni et al. 2007) have been widely used for neuroimaging. However, these clinical or ‘human-scale’ imaging modalities often lack the resolution to spatially and temporally resolve underlying neuronal processes. Therefore, investigators circumvented this drawback by utilizing pre-clinical animal models in conjunction with imaging methods capable of high spatial and temporal resolution.

The availability of an ever-increasing spectrum of optical contrast agents (Zhang et al. 2002), and technical advances in optics (Kerr et al. 2008, Tye et al. 2012), coupled with optogenetic constructs for manipulating neuro-circuitry (Tye et al. 2012), have resulted in optical neuroimaging becoming the tool of choice for neuroscientific applications. Moreover, these optical neuroimaging techniques permit cellular-scale spatial resolution and millisecond temporal resolution (Kerr et al. 2008).

Much of today’s optical neuroimaging is performed using sophisticated optics and cumbersome electronic hardware (Theer et al. 2003). The bulky nature of such setups requires the animal to be anesthetized and restrained stereotactically, greatly limiting the types of experiments that can be performed *in vivo* and at multiple time points. Additionally, the use of anesthetics has been found to alter the baseline physiology of the brain during *in vivo* imaging (Bonhomme et al. 2011). Therefore, miniaturization of the imaging hardware in conjunction with the ability to image the brains of awake and unanesthetized animals would circumvent these issues.

Recent advances in miniaturized optics and electronic devices (Theuwissen 2008) paved way for the “next generation” optoelectronic systems capable of unique real-time, awake optical imaging. Fig. 1 shows the evolution of neuroimaging systems from benchtop setups to ‘head-mounted’ platforms. It is not always necessary to miniaturize the entire system. As shown in Fig. 1, depending on the type of experiment, individual elements of the imaging system can be modified to match the required level of animal mobility. This can range from having the animal’s head affixed while the animal pedals on a moving ball (Dombeck et al. 2007), to systems that allow unrestrained animal mobility (Ghosh et al. 2011). It is worth noting that similar technical advances were also responsible for the development of ‘implantable’ microimagers (Ng et al. 2008). These implantable devices are image sensor array chips that have been packaged into ‘ready-to-use’ modules. Recent work has elegantly demonstrated their utility in applications ranging from neural imaging (Ng et al. 2008) to blood-flow imaging in freely moving rats (Haruta et al. 2014). However, the focus of the current review is on non-implantable imagers. An excellent recent review by Kerr and Nimmerjahn focused on functional imaging at the cellular level and primarily covered imaging approaches that utilized exogenous contrast agents (Kerr et al. 2012). In this review, we examine miniaturized neuroimaging systems that utilize exogenous contrast agents, e.g. wide-field fluorescence imaging (Ferezou et al. 2006, Flusberg et al. 2008), two-photon

fluorescence imaging (Helmchen et al. 2001, Sawinski et al. 2009), as well as those that exploit intrinsic optical properties of biological tissues, e.g. multispectral imaging and blood flow based laser speckle imaging systems (Liu et al. 2013). Finally, we discuss the relative advantages and disadvantages of each approach and the exciting prospects of this technology from the micro- (i.e. cellular) to the macro-scale (i.e. whole tissue) for neuroimaging.

## Miniaturized optical systems based on exogenous contrast agents

Optical contrast agents permit visualization of underlying microvasculature (Bassi et al. 2011) as well as functional cellular dynamics such as membrane potentials (Mutoh et al. 2011) and intercellular calcium concentrations (Mittmann et al. 2011). Conjugation of fluorescent dyes with genetically encoded biomarkers/target molecules (Chalfie et al. 1994), as well as their ability to shift emission spectra in response to biological perturbations (McVea et al. 2012) has enabled fluorescent imaging to be utilized in a wide range of applications (Petersen et al. 2003, Mank et al. 2008). Although variability in contrast agent delivery or unstable gene expression can affect the emitted fluorescence, an ever increasing array of fluorescent dyes with different excitation spectra, better quantum yields and extinction coefficients has greatly enhanced our ability to simultaneously monitor a multitude of targets and neurophysiologic processes.

Miniaturization of fluorescent microscopy was first attempted by using an optic fiber bundle to relay the emitted fluorescent light as well as the high intensity excitation illumination to and from a standard benchtop system (Helmchen et al. 2001). However, recent technological breakthroughs have enabled additional miniaturization of fluorescent microscopy systems as discussed below. A summary of miniaturized and mobile brain imaging platforms from the recent literature can be found in Table 1.

### Single-Photon Microscopy Systems

Since single-photon microscopy does not need an expensive near-infrared laser or a laser scanning mechanism, it is less complicated and more affordable than two-photon microscopy. These advantages also make it well-suited for miniaturized optical neuroimaging applications. The absence of a laser scanning mechanism endows single-photon microscopy with a high temporal resolution that is suitable for imaging dynamic neurobiological phenomena. However, single-photon systems can only acquire two dimensional images and the use of wide-field excitation increases the risk of photo-bleaching the sample.

Ferezou et al. were one of the first to report *in vivo* fluorescent imaging in freely moving animals (Ferezou et al. 2006). In their system, a customized multi-fiber array (Fig. 2a) placed in direct contact with the rat whisker barrel cortex relayed emission and excitation light to and from a standard benchtop epifluorescence imaging system. A voltage sensitive dye (RH1691) was employed for functional imaging of the barrel cortex following whisker stimulation. The dye primarily stained layer 2/3 sensory neurons. The system had a temporal resolution of 2 ms and covered a 3 mm × 3 mm field of view (FOV). Spatial resolution was limited by the size of individual fibers in the fiber optic bundle as well as by the low numerical aperture due to the absence of an objective lens at the specimen-optical fiber

interface. While the exact spatial resolution of the system was not reported, the authors could successfully visualize the barrel cortex at sub-columnar resolution. Images from the fiber optic microscope were compared with those from a conventional fluorescent imaging setup, and no significant differences in peak fluorescence amplitude, duration or spatial extent of the sensory response to whisker stimulation were observed. Furthermore, the sensory response to whisker stimulation in rats anesthetized with isoflurane was compared to that of awake rats. The authors showed that awake animals exhibited a response longer in duration and larger in spatial extent than their anesthetized counterparts (Ferezou et al. 2006).

Murayama et al. (Murayama et al. 2007) reported a single-photon fiber optic system for recording dendritic calcium signals (Fig. 2b). To illuminate and collect light locally from the distal dendrites of cortical layer 5 neurons, an optic fiber was directly inserted into layer 5 of the rat's brain. To acquire different views of the dendrites, two optical set-ups were employed: the first included a one-fiber system for a side-on view; and the second was a two-fiber system for imaging above the cortex. The one-fiber system was tested on freely moving rats. After injecting a calcium-sensitive dye (Oregon Green 488 BAPTA-1), calcium signals were recorded from layer 5 neurons in stationary and free moving states, as well as during whisker stimulation. The amplitude of the calcium signals was observed to vary with the state of the animals. Furthermore, the authors simulated the effects of motion on their image acquisition by using a bench top stirrer assembly to vibrate an anesthetized rat while the microscope continuously acquired images. No significant changes were observed in the fluorescent signal from calcium transients. A later publication using the same system investigated dendritic calcium changes in layer 5 pyramidal cells of the somatosensory cortex in rats following sensory stimulation (Murayama et al. 2009). Their results showed that the strength of sensory stimulation was encoded in the calcium response of local layer 5 pyramidal cells in a graded manner.

Flusberg et al. (Flusberg et al. 2008) reported a miniaturized single-photon microscope for cellular-level imaging at frame rates up to 100 Hz. The optical components of the microscope consisted of a compact coupling assembly, focusing mechanism and two separate objective lenses. The head-mounted microscope weighed only 1.4 g and had a spatial footprint on the scale of a centimeter (Fig.2c). This ensured that the microscope could be easily supported by an adult mouse. The head piece was then connected to a standard benchtop fluorescent imaging system. Dual objective lenses ensured that both superficial and deep tissue could be imaged. Limitations in packing density and number of individual fibers in the optic fiber bundle restricted the lateral resolution and FOV to ~2.8–3.9  $\mu\text{m}$  and ~240–370  $\mu\text{m}$ , respectively. Its 75 Hz data acquisition rate made it possible to discern the movement of individual erythrocytes within blood vessels. Tests on freely moving mice revealed that motion artifacts were limited to less than 2  $\mu\text{m}$  of lateral displacement. The microscope was used to record surface blood flow in the mouse neocortex and in the CA1 region of the hippocampus. Using temporal cross-correlation analysis, the authors demonstrated that blood flow velocities varied greatly among capillaries, venules and arterioles. The microscope was also used to compare Purkinje cell dendritic  $\text{Ca}^{2+}$  dynamics during the anesthetized and mobile states. Purkinje cells exhibited larger  $\text{Ca}^{2+}$  spike rates during locomotion than at rest. Additionally, correlation analysis of  $\text{Ca}^{2+}$  spiking

between pairs of Purkinje cells revealed larger correlation coefficients during active movements than at rest.

Cha et al. (Cha et al. 2014) designed a fiber-optic fluorescence microscope that used an objective focusing lens consisting of two symmetric aspheric lenses covering a  $\sim 4 \text{ mm}^2$  FOV. Their fiber optic bundle interfaced with a standard benchtop based fluorescence system. *In vitro* imaging demonstrated that this system was capable of resolving astrocytes and pyramidal cells in a mouse brain section, and image quality was comparable to that of a conventional fluorescence microscope. *In vivo* experiments with this system were conducted on head-restrained, awake mice placed on a treadmill. Using this microscope, the authors were able to demonstrate that Bergmann glia in the cerebellum showed larger amplitude of  $\text{Ca}^{2+}$  signals during locomotion than when the animal was at rest.

The ‘next-generation’ neuroimaging systems were fully miniaturized by using surface mount light emitting diodes (LEDs) for excitation illumination and minute ( $\sim 3 \text{ mm} \times 3 \text{ mm}$ ) CMOS image sensors for image acquisition. These miniaturized microscopes enabled a transformation of the experimental paradigm from one in which restrained animals were imaged, to one in which interacting or naturally behaving animals could be imaged.

Osman/Park et al. (Osman et al. 2011, Park et al. 2011, Osman et al. 2012) designed a neuroimaging system with a miniaturized illumination source, focusing optics and image sensor (Fig.2d). This microscope featured a frame rate of 500 frames per second (fps) and a sensitivity of 0.1% of the initial fluorescent signal (0.1% F/F). Weighing 10 g, the system had a FOV of  $\sim 4.8 \text{ mm}^2$ , lateral resolution of  $25 \mu\text{m}$  and a 1.8 magnification ratio. Without a physical shutter, the system required very stable illumination to precisely control the exposure time. Therefore, the LED output was actively controlled by a photodiode and microcontroller to maintain light intensity within 0.2 % deviation of its mean intensity. Small changes ( $< 1\%$  F/F) in barrel cortical fluorescence signals due to whisker stimulation were detectable using a voltage sensitive dye (RH1691). As reported in (Osman et al. 2012), the resulting signal quality was comparable to that of a benchtop fluorescent microscope equipped with a Red-Shirt-Imaging camera (Decatur, GA). However, this microscope was not a fully miniaturized prototype. The image acquisition controller was a non-miniaturized field-programmable gate array (FPGA) assembly with an electric wire bundle connected to the head piece. The microscope’s use is limited because the tether’s rigidity could affect the animal’s mobility in certain kinds of functional experiments.

Ghosh et al. (Ghosh et al. 2011) designed a similarly miniaturized fluorescence microscope (Fig. 2e). Weighing only 1.9 g, it could be easily carried by an adult mouse. A maximum FOV of  $600 \times 800 \mu\text{m}$  was reported while supporting a magnification ratio of 5.0 and a lateral resolution of  $\sim 2.5 \mu\text{m}$ . The microscope was capable of high-speed cellular level imaging up to a frame rate of 100 Hz while covering a FOV of  $\sim 0.5 \text{ mm}^2$ . Using this system, synaptic activation via calcium tracking in up to 206 Purkinje neurons from nine cerebellar microzones was reported. The microscope was first used to study the microcirculation during mobile and rest states of mice. The authors reported an increase in erythrocyte flow speeds when the animals transitioned from rest to locomotion states. Additional studies were focused on differentiating synaptic dynamics of freely moving mice during different

behavioral states using a fluorescent calcium indicator. The authors showed that mean spike rates increased as the animal transitioned from rest to groom to locomotion states, respectively (Ghosh et al. 2011). When compared to the fiber-optic-based microscope previously reported by the same group (Flusberg et al. 2008), the new microscope showed better performance in terms of optical resolution, fluorescence signal quality and system robustness. The FOV of the fiber-bundle-based microscope was restricted by the maximum diameter and bending radius of the bundle, while the FOV in this new microscope was only limited by sensor size and the focusing optics. Additionally, the fiber bundle microscope exhibited drastic attenuation of the transmitted fluorescent light due to bending and light absorption of the fiber. The fluorescence detected by the sensor increased from ~20% – 95% while a ~700% greater FOV was achieved. No realignment of the optics was necessary between imaging sessions, and the imaging duration could be extended up to 45 min. Observed motion artifacts were limited to less than 1  $\mu\text{m}$  even when imaging running animals.

O'Sullivan et al. (O'Sullivan et al. 2013) reported the fabrication of a miniature, integrated semiconductor-based fluorescence sensor, designed for detecting fluorophores and tumor-targeted molecular probes (Fig. 2f). The system consisted of multiple vertical-cavity surface-emitting laser (VCSEL) dies as the excitation source, GaAs photodiodes as two point detectors, and a CMOS (Complementary Metal Oxide Semiconductor) ROIC (Read-out Integrated Circuit) for reading out the data, mounted on a custom printed circuit board (PCB). A standard 18-pin connector was employed for data transmission. The system was extremely lightweight (~0.7 g) with a small footprint (~1  $\text{cm}^3$ ). VCSEL excitation wavelengths were optimized for the Cy 5.5 dye, and the emission filter was directly coated on to the custom-made image sensor. The onboard photocurrent ranged from 5 pA to 15 nA and was amplified and digitized using the ROIC for subsequent data acquisition. When the system was tested on freely moving mice, the authors reported an increase of ~ 500 pA in the photocurrent following injection of Cy 5.5 fluorescence dye. This miniaturized system required precise positioning and fixation to the targeted object, which made it difficult to use on soft tissue or when imaging small targets (O'Sullivan et al. 2013).

## Two-Photon Microscopy Systems

Two-photon microscopy (2PM) uses ultra-short pulses of a long wavelength laser to scan biological tissue in three dimensional space, creating a depth resolved image stack. This approach excites only the voxel being imaged, thereby minimizing photo-toxicity. Additionally, the use of a longer wavelength excitation light reduces scattering in biological tissues, enabling deeper imaging depths. Nonetheless, laser scanning impacts the acquisition frame rate, enabling only relatively slow phenomena to be imaged. Also, the laser scanning pattern can be distorted by the motion of awake, unrestrained animals. Due to the high power and temporal modulation accuracy required of the laser, miniaturized 2PM systems utilize a standard benchtop 2PM system retrofitted with an optical fiber bundle and focusing optics, to deliver excitation and collect the emitted light from the freely moving animal.

Helmchen et al. reported the first miniaturized head-mounted two photon microscope (Helmchen et al. 2001). The head piece consisted of a single-mode optical fiber for

excitation, a miniature scanning device, microscope optics and a miniature photo multiplier tube (PMT) (Fig. 3a). Two-dimensional scanning was realized by resonant scanning in a Lissajous pattern. A line scanning mode was also available for faster imaging. The microscope was 7.5 cm high, 25 g in weight and could be supported by an adult rat. *In vivo* imaging on anesthetized rats injected with a dextran dye showed surface blood vessels and the underlying capillary network. The maximum imaging depth was 250  $\mu\text{m}$ . Furthermore, imaging on anesthetized rats injected with a calcium indicator (calcium green-1) resolved dendritic processes in layer 2/3 neurons. Testing this microscope on freely moving animals, the authors determined that rapid turning of the head and sudden contact with a wall induced noticeable motion artifacts in the acquired fluorescence images.

A two-photon microscope with two objective gradient-index (GRIN) lenses for miniaturized focusing was built by Gobel et al. (Göbel et al. 2004). Pre-compensation for the broadening of excitation light within the optic fiber was achieved by pre-chirping the laser pulses. Lateral and axial resolutions of 2.5  $\mu\text{m}$  and 20  $\mu\text{m}$ , respectively, were achieved. The pixelated image was smoothed with a Gaussian filter to compensate for the 1  $\mu\text{m}$  spacing between individual fibers in the optic fiber bundle, which also reduced image contrast. As proof of concept for the device, *in vivo* imaging of fluorescein-injected, anesthetized rats was performed to visualize blood vessels.

Piyawattanametha et al. (Piyawattanametha et al. 2009) reported a portable 2PM microscope based on a microelectromechanical systems (MEMS) laser scanning mirror (Fig. 3b). The system weighed 2.9 g. Moreover, the implantation of the MEMS scanner made the 2PM system more compact, i.e. 2 cm $\times$ 1.9 cm $\times$ 1.1 cm in size. Separate optical fibers for fluorescence collection and excitation pulse delivery were utilized. The system had transverse and axial resolutions of 1.29 $\pm$ 0.05  $\mu\text{m}$  and 10.3 $\pm$ 0.3  $\mu\text{m}$ , respectively, with a maximum FOV of 295 $\times$ 100  $\mu\text{m}$  and was used to image neocortical capillaries in mice injected with fluorescein dye. In the line scanning mode, individual erythrocytes inside blood vessels could be tracked in an anesthetized animal.

Sawinski et al. (Sawinski et al. 2009) reported a miniaturized head-mounted 2PM system for recording  $\text{Ca}^{2+}$  transients from the somata of layer 2/3 neurons in the visual cortex of awake, freely moving rats (Fig. 3c). As described by the authors, 'a custom designed water-immersion lens and a leveraged non-resonant fiber scanner were employed, providing greater control over the scan pattern than resonant scanning' (Sawinski et al. 2009). Their multi-lens setup provided higher excitation and detection numerical apertures (NA) compared to using a single GRIN lens. Besides neuronal activity resulting from visual stimuli, bending of the optical fiber also caused fluctuations in the detected fluorescence signals. To counteract this, two fluorescent dyes, a green calcium indicator (Oregon green BAPTA-1, OGB1) and sulforhodamine 101 (SR101) were employed. Since SR101 fluorescence was not related to neuronal activity, it was used to normalize the signal from the green fluorescent calcium indicator. They conducted one of the first *in vivo* experiments on freely moving animals on a semicircular track. They placed three monitors with different visual stimuli at the apex and the ends of the track. The experiment was conducted in the dark except for light stimulation from the monitors. Synchronized infrared videos were recorded during the experiment to investigate the relationship between animal movement

and calcium indicator signals. A significant increase in calcium transients was observed when the animal swept its gaze across the visual stimuli. It should be noted that motion artifacts were observed during chewing and head movement of the animals. Of these, lateral displacements were corrected by an automated algorithm as described in (Greenberg et al. 2009).

Barretto et al. (Barretto et al. 2009) designed a micro-lens-based 2PM imager. By combining a GRIN lens with a plano-convex lens, their set-up was corrected for aberration and had a higher numerical aperture than just using the GRIN lens by itself. In vivo images of GFP-expressing pyramidal cells in region CA1 of the mouse hippocampus showed better resolution than images acquired using the GRIN lens alone. Finally, Helmchen et al. provide a detailed protocol for investigators interested in designing their own bespoke two-photon microscopy based systems for in vivo imaging in freely moving animals in (Helmchen et al. 2013). The dissemination of such hardware ‘recipes’ using commercially available components should make imaging in awake animals more widespread.

The feasibility of other approaches, such as diffuse optical tomography (Holzer et al. 2006), light-sheet-based microscopy (Engelbrecht et al. 2010) and two-photon microendoscopes (Flusberg et al. 2005, Saunter et al. 2012) have also been demonstrated in freely moving animals. Besides the abovementioned applications, head-mounted microscopes have also been used for studying cortical calcium waves in newborn mice (Adelsberger et al. 2005), and for imaging hippocampal cells during virtual navigation tasks (Dombeck et al. 2007, Dombeck et al. 2010).

## Miniaturized optical systems based on endogenous contrast

The earliest form of intrinsic contrast based optical imaging was performed using multispectral imaging, which exploits the spectral properties of oxygenated and deoxygenated hemoglobin to visualize the relative oxygen saturation in biological tissue (Hillman 2007). Recently, laser speckle contrast imaging (LSCI), that relies on flowing blood for image contrast (Rege et al. 2012), has also been miniaturized for freely moving animal experiments (Table 1).

### Multispectral Imaging System

Multispectral imaging has a long and established history in neuroscience (Ts’o et al. 1990). However, it lacks complementary contrast from other tissue structures because it does not rely on any exogenous contrast agents, but rather on the spectrally dependent absorption properties of hemoglobin moieties (Murari et al. 2007). Nonetheless, miniaturized multispectral imaging provides a convenient way to observe tissue oxygenation changes in the brain.

Murari et al. (Murari et al. 2009) (Murari et al. 2010) designed a microscope with the potential for multi-modality neuroimaging. This system occupied  $\sim 4 \text{ cm}^3$  and weighed 5.4 g, while incorporating a highly sensitive custom-made CMOS camera. Cortical blood vessels 15–20  $\mu\text{m}$  diameter could be visualized using this system. *In vivo* experiments on rats using a green LED light source demonstrated a reflectance change between the active state and

rest state. Tests on fluorescence, LSCI and multispectral imaging, demonstrated the feasibility of developing a multi-modality miniaturized microscope for neuroimaging applications.

### Laser Speckle Contrast Imaging System

Laser Speckle Contrast Imaging (LSCI) relies on the statistical properties of coherent light scattered by red blood cells (RBCs) moving inside perfused blood vessels. A higher blood flow velocity generates a greater speckle blur and a lower speckle contrast and vice versa. This mechanism enables LSCI to assess relative blood flow changes as well as delineate microvascular structure from background tissue with a high contrast-to-noise ratio (Senarathna et al. 2013). However, LSCI typically requires an image stack to compute relative blood flow maps, thereby limiting its intrinsic temporal resolution.

Miao et al. (Miao et al. 2011) designed a head-mounted microscope for laser speckle contrast imaging (Fig. 4). The microscope was ~20 g in weight and 3.1 cm in height. This head-mounted system consisted of a miniature macrolens system, image sensor, optical fiber bundle and circuits. The spatial resolution achievable was 16 lp/mm with less than 2% distortion. To eliminate motion artifacts, registered laser speckle contrast analysis (rLASCA) was applied to the raw speckle data, wherein each image from the image stack was aligned with the first image. While the rat was free moving, blood vessels approximately 4 pixels or ~50  $\mu\text{m}$  in diameter could be identified (Fig. 4). This spatial resolution was comparable to that of standard benchtop laser speckle imaging systems and suitable for studying the cerebral blood flow (CBF) of major vessels under different physiological conditions (Miao et al. 2011). Liu et al. (Liu et al. 2013) designed a dual-modality LSCI/multispectral microscope, also extendable for fluorescence imaging (Fig. 4b). The multi-modal microscope weighed 1.5 g, and the internal optical components were adjustable, providing different magnification ratios and FOVs. They conducted an extensive study on cortical spreading depression (CSD) in freely moving and anesthetized animals. Hemodynamic parameters were calculated from simultaneously acquired LSCI and dual-wavelength multispectral imaging data. The authors demonstrated that there was a significant difference in CSD propagation latencies between anesthetized and awake animals (Fig. 4b). CSD in isoflurane-anesthetized rats was significantly longer in duration, and agreed with previous studies demonstrating that anesthetics extend CSD duration and reduce CSD frequency (Kudo et al. 2008). Senarathna et al. (Senarathna et al. 2011, Senarathna et al. 2012) reported the development of a miniaturized LSCI microscope weighing 7 g and occupying less than 5  $\text{cm}^3$  (Fig. 4c). The system consisted of a laser diode (tri-wavelength), focusing optics, CMOS sensor, with control circuits housed in a backpack. The tetherless setup made the microscope suitable for behavioral tests in freely moving rodents. LSCI images could be computed following acquisition of 240 raw speckle images. By converting speckle contrast to the correlation time of blood flow (Duncan et al. 2008), relative CBF maps were generated (Fig. 4c). As reported in (Senarathna et al. 2012), image quality degraded an hour after implantation. The authors concluded that this might be attributable to the refractive index matching material (i.e. mineral oil) gradually evaporating and the thinned skull optical window preparation eventually drying out. Also the use of a rolling shutter technique for exposure time control together with a relatively low frame rate of 6 fps, resulted in long

exposure times that averaged out some of the speckle contrast. The spatial resolution of the system was 20  $\mu\text{m}$ , which was the pixel size of the image sensor. Higher spatial resolution could be achieved by replacing it with a smaller pixel size CMOS sensor.

## Discussion

Miniaturized brain imaging systems, while having the advantages of portability, size, and multimodality neuroimaging in awake/unrestrained animals are prone to several shortcomings. Therefore, the decision to utilize such an imaging system instead of a benchtop setup should be based on a balance of its strengths and weaknesses.

A major concern with miniaturized neuroimaging systems is the additional weight it imposes on the animal. While a benchtop system tethered to an animal via an optical fiber bundle imposes minimal additional weight, a fully miniaturized system requires the entire weight of the imaging system be borne by the animal. Hence, it is vital that such imaging systems are designed with critical weight limits for the applications under consideration. A similar argument applies to the spatial footprint of the device attached to the animal's head, including the total height and size of the instrumentation. Use of a larger species of animals, e.g. rats versus mice, might partially obviate this concern. Nonetheless, it is crucial that experimental protocols involving miniaturized, head-mounted microscopes clearly establish that the animal behavior under study is not significantly affected by the implanted or mounted neuroimaging system (Sawinski et al. 2009).

Increased motion artifacts are another concern with studies in freely moving, unanesthetized animals. Beyond respiration and cardiac motion artifacts that are seen in benchtop imaging, miniaturized imaging platforms are susceptible to motion caused by whole-body movement as well as relative motion between the head-mounted microscope and the animal's body. Some imaging modalities are more sensitive to motion than others, e.g. 2PM suffers more from motion artifacts than wide-field fluorescence microscopy. Different image registration and motion removal algorithms can be employed to enhance image quality (Dombeck et al. 2009).

A frequently overlooked aspect of miniaturized imaging systems is the challenge of building them from high-performance optical and electronic components in view of their size, weight and power constraints. Therefore, due to limitations in current hardware and optical component fabrication, compact imaging systems usually offer 'bare-bones' imaging capabilities that are customized to a given experimental paradigm. In doing so, such systems lack the imaging precision, accuracy and flexibility of conventional benchtop systems. For example, in miniaturized LSCI systems, the VCSEL laser source may emit laser light that is not very coherent, thereby degrading speckle contrast. While a benchtop setup can be easily focused, the magnification changed and multiple wavelengths imaged conveniently, a miniaturized neuroimaging system has limited focusing ability, a fixed magnification level and imaging different wavelengths is often challenging. Therefore, flexibility and precision need to be considered before choosing a miniaturized neuroimaging system over a conventional benchtop imaging system.

An important aspect of imaging in awake, freely moving animals is correlating their behavior with their neural responses. Different types of monitoring tools have been employed to monitor animal activity for various applications. Typically, synchronized videos are recorded during experiments measuring neural response to document the animal's behavior. In (Sawinski et al. 2009), the positions of four infrared LEDs attached to the microscope were used to determine animal's movements and orientation of its head. By correlating the animal's behavior with visual stimuli presented on monitors in its field of view, the authors were able to study the relationship between visual perturbations and concurrently recorded calcium signals. In (Dombeck et al. 2007), running speeds were measured by the rotation of a spherical treadmill on which the animal was placed and infrared videos were recorded to catalog grooming and whisking behavior. The changes in the fluorescence trace of neurons labeled with calcium sensitive dye during running behavior were analyzed, with a significant fraction of neurons exhibiting a strong running correlation. As reported by the authors, transients of some neurons mimicked the time course of running speed.

While in their simplest form many head mounted optical microscopes have utilized a single imaging modality, integrated systems with two imaging modalities have begun to emerge. Most commonly, multispectral imaging, given its relative simplicity in implementation, is combined with another modality such as fluorescent or speckle imaging (Murari et al. 2010, Liu et al. 2013). Such systems provide scientists access to a multitude of biological variables enabling them to obtain a more holistic view of the neurobiology of awake and freely moving animals. Moving forward, given the need for acquiring multi-parametric data, the development of miniaturized systems with more than two imaging modalities may become commonplace.

Combining optical imaging with other neurobiological data such as electrophysiology (Szuts et al. 2011), biochemical recordings etc., could lead to a multimodality system for studying the brains of freely moving animals. For example, visualizing cellular calcium dynamics with fluorescent imaging while simultaneously monitoring electrophysiology with a transparent electrocorticographic (ECoG) sensor array (Ledochowitsch et al. 2011), could herald a new era of neurobiological investigation. Or one could envision experiments involving functional neuromodulation via electrical or optogenetic stimulation to assess interactions between stimulation and neuroimaging.

## Conclusions and future directions

In the past decade, traditional benchtop based microscopy of anesthetized and constrained animals has slowly made way to neuroimaging in freely moving animals. Technological innovations in electronic hardware, miniaturized optics and computing power have converged to make this tremendous advance possible. This has brought about a paradigm shift in neuroscience, enabling scientific investigations geared towards uncovering natural brain function and dysfunction due to disease. Since optical imaging is relatively simple to operate in contrast to other imaging modalities such as ultrasound, MRI etc., the construction of miniaturized neuroimaging platforms has experienced an exponential growth (Table 1).

Early instrumentation for brain imaging in freely moving animals involved a standard benchtop microscope coupled to an optical fiber bundle that attached to an optical window over the animal's intact brain. The next generation of neuroimaging systems utilized optics inserted in to the animal's head-mount, while keeping the rest of the microscope assembly unchanged. However, in the latest generation of neuroimaging systems, the development of miniaturized light sources and sensitive CMOS image sensors within the head-mounted microscope is making the need for optical fiber bundles less critical. Nonetheless, such imaging systems still require wires to connect the head-mounted instrumentation with advanced control circuitry on the benchtop, thus tethering the animal. Fully compact microscope systems that utilize miniature control and storage electronics encased in a backpack worn by the animal have begun to emerge, enabling truly tetherless animal brain imaging. With impending improvements in electronic and optical design, supported by the availability of sophisticated computer aided design (CAD) and rapid prototyping tools, fully mobile and ultra-compact head mounted systems can be envisioned. These will increase user convenience and make possible a range of experiments that were previously unfeasible due to the presence of tethers. Examples include behavioral experiments involving complex maze structures as well as group studies wherein brain function of multiple freely interacting animals can be simultaneously tracked as an ensemble.

Future applications of miniaturized microscopes need not be limited to conventional neuroscience applications, but could include imaging in a wide array of preclinical disease models. For example, one could envisage the use of head mounted optical microscopes for 'lifetime' imaging of brain tumor progression, or sudden onset/termination of seizures; imaging of neurovascular coupling, imaging neural plasticity or continuous imaging of the etiology of stroke. In summary, miniaturized optical head-mounted imaging systems have progressed considerably from their benchtop antecedents. We envision a future in which the use of such portable, user-friendly systems will become commonplace in neuroscience laboratories alongside advances in optogenetics and high-throughput electrophysiology. It is our belief that miniaturized optical neuroimaging in unrestrained animals will be a critical ingredient of the next-wave of breakthroughs in the neurosciences and investigations of brain-related pathologies.

## Acknowledgments

Supported by NCI 1R21CA175784-01.

## References

- Adelsberger H, Garaschuk O, Konnerth A. Cortical calcium waves in resting newborn mice. *Nat Neurosci.* 2005; 8(8):988–990. [PubMed: 16007081]
- Barretto RP, Messerschmidt B, Schnitzer MJ. In vivo fluorescence imaging with high-resolution microlenses. *Nat Methods.* 2009; 6(7):511–512. [PubMed: 19525959]
- Bassi A, Fieramonti L, D'Andrea C, Mione M, Valentini G. In vivo label-free three-dimensional imaging of zebrafish vasculature with optical projection tomography. *J Biomed Opt.* 2011; 16(10):100502. [PubMed: 22029341]
- Bonhomme V, Boveroux P, Hans P, Brichant JF, Vanhauzenhuysse A, Boly M, Laureys S. Influence of anesthesia on cerebral blood flow, cerebral metabolic rate, and brain functional connectivity. *Curr Opin Anaesthesiol.* 2011; 24(5):474–479. [PubMed: 21772143]

- Cha, J., Paukert, M., Bergles, DE., Kang, JU. Fiber optic fluorescence microscopy for functional brain imaging in awake mobile mice. SPIE BiOS, International Society for Optics and Photonics; 2014.
- Chalfie M, Tu Y, Euskirchen G, Ward WW, Prasher DC. Green fluorescent protein as a marker for gene expression. *Science*. 1994; 263(5148):802–805. [PubMed: 8303295]
- Cianfoni A, Colosimo C, Basile M, Wintermark M, Bonomo L. Brain perfusion CT: principles, technique and clinical applications. *Radiol Med*. 2007; 112(8):1225–1243. [PubMed: 18074193]
- Dombeck DA, Graziano MS, Tank DW. Functional clustering of neurons in motor cortex determined by cellular resolution imaging in awake behaving mice. *The Journal of Neuroscience*. 2009; 29(44):13751–13760. [PubMed: 19889987]
- Dombeck DA, Harvey CD, Tian L, Looger LL, Tank DW. Functional imaging of hippocampal place cells at cellular resolution during virtual navigation. *Nat Neurosci*. 2010; 13(11):1433–1440. [PubMed: 20890294]
- Dombeck DA, Khabbaz AN, Collman F, Adelman TL, Tank DW. Imaging large-scale neural activity with cellular resolution in awake, mobile mice. *Neuron*. 2007; 56(1):43–57. [PubMed: 17920014]
- Duncan DD, Kirkpatrick SJ. Can laser speckle flowmetry be made a quantitative tool? *JOSA A*. 2008; 25(8):2088–2094. [PubMed: 18677371]
- Engelbrecht CJ, Voigt F, Helmchen F. Miniaturized selective plane illumination microscopy for high-contrast in vivo fluorescence imaging. *Optics Letters*. 2010; 35(9):1413–1415. [PubMed: 20436587]
- Ferezou I, Bolea S, Petersen CC. Visualizing the cortical representation of whisker touch: voltage-sensitive dye imaging in freely moving mice. *Neuron*. 2006; 50(4):617–629. [PubMed: 16701211]
- Flusberg BA, Jung JC, Cocker ED, Anderson EP, Schnitzer MJ. In vivo brain imaging using a portable 3.9 gram two-photon fluorescence microendoscope. *Optics letters*. 2005; 30(17):2272–2274. [PubMed: 16190441]
- Flusberg BA, Nimmerjahn A, Cocker ED, Mukamel EA, Barretto RP, Ko TH, Burns LD, Jung JC, Schnitzer MJ. High-speed, miniaturized fluorescence microscopy in freely moving mice. *Nat Methods*. 2008; 5(11):935–938. [PubMed: 18836457]
- Ghosh KK, Burns LD, Cocker ED, Nimmerjahn A, Ziv Y, Gamal AE, Schnitzer MJ. Miniaturized integration of a fluorescence microscope. *Nat Methods*. 2011; 8(10):871–878. [PubMed: 21909102]
- Göbel W, Kerr JN, Nimmerjahn A, Helmchen F. Miniaturized two-photon microscope based on a flexible coherent fiber bundle and a gradient-index lens objective. *Optics letters*. 2004; 29(21):2521–2523. [PubMed: 15584281]
- Greenberg DS, Kerr JN. Automated correction of fast motion artifacts for two-photon imaging of awake animals. *Journal of neuroscience methods*. 2009; 176(1):1–15. [PubMed: 18789968]
- Haruta M, Kitsumoto C, Sunaga Y, Takehara H, Noda T, Sasagawa K, Tokuda T, Ohta J. An implantable CMOS device for blood-flow imaging during experiments on freely moving rats. *Japanese Journal of Applied Physics*. 2014; 53(4)
- Heeger DJ, Ress D. What does fMRI tell us about neuronal activity? *Nat Rev Neurosci*. 2002; 3(2):142–151. [PubMed: 11836522]
- Helmchen F, Denk W, Kerr JN. Miniaturization of two-photon microscopy for imaging in freely moving animals. *Cold Spring Harbor Protocols*. 2013; 2013(10) pdb. top078147.
- Helmchen F, Fee MS, Tank DW, Denk W. A miniature head-mounted two-photon microscope: high-resolution brain imaging in freely moving animals. *Neuron*. 2001; 31(6):903–912. [PubMed: 11580892]
- Hillman EM. Optical brain imaging in vivo: techniques and applications from animal to man. *J Biomed Opt*. 2007; 12(5):051402–051402. 051428. [PubMed: 17994863]
- Holzer, M., Schmitz, C., Pei, Y., Graber, H., Abdul, RA., Barry, J., Muller, R., Barbour, R. 4D functional imaging in the freely moving rat. *Engineering in Medicine and Biology Society, 2006; EMBS'06. 28th Annual International Conference of the IEEE; IEEE*. 2006.
- Jones PB, Shin HK, Boas DA, Hyman BT, Moskowitz MA, Ayata C, Dunn AK. Simultaneous multispectral reflectance imaging and laser speckle flowmetry of cerebral blood flow and oxygen metabolism in focal cerebral ischemia. *J Biomed Opt*. 2008; 13(4):044007–044007. 044011. [PubMed: 19021335]

- Kerr JN, Denk W. Imaging in vivo: watching the brain in action. *Nat Rev Neurosci.* 2008; 9(3):195–205. [PubMed: 18270513]
- Kerr JN, Nimmerjahn A. Functional imaging in freely moving animals. *Curr Opin Neurobiol.* 2012; 22(1):45–53. [PubMed: 22237048]
- Kudo C, Nozari A, Moskowitz MA, Ayata C. The impact of anesthetics and hyperoxia on cortical spreading depression. *Experimental neurology.* 2008; 212(1):201–206. [PubMed: 18501348]
- Ledochowitsch, P., Olivero, E., Blanche, T., Maharbiz, MM. A transparent  $\mu$ ECoG array for simultaneous recording and optogenetic stimulation. *Engineering in Medicine and Biology Society; EMBC, 2011 Annual International Conference of the IEEE; IEEE.* 2011.
- Liu R, Huang Q, Li B, Yin C, Jiang C, Wang J, Lu J, Luo Q, Li P. Extendable, miniaturized multimodal optical imaging system: cortical hemodynamic observation in freely moving animals. *Optics Express.* 2013; 21(2):1911–1924. [PubMed: 23389174]
- Mank M, Santos AF, Drenth S, Mrcic-Flogel TD, Hofer SB, Stein V, Hendel T, Reiff DF, Levelt C, Borst A. A genetically encoded calcium indicator for chronic in vivo two-photon imaging. *Nature Methods.* 2008; 5(9):805–811. [PubMed: 19160515]
- McVea DA, Mohajerani MH, Murphy TH. Voltage-sensitive dye imaging reveals dynamic spatiotemporal properties of cortical activity after spontaneous muscle twitches in the newborn rat. *The Journal of Neuroscience.* 2012; 32(32):10982–10994. [PubMed: 22875932]
- Miao P, Lu H, Liu Q, Li Y, Tong S. Laser speckle contrast imaging of cerebral blood flow in freely moving animals. *J Biomed Opt.* 2011; 16(9):090502. [PubMed: 21950906]
- Mittmann W, Wallace DJ, Czubayko U, Herb JT, Schaefer AT, Looger LL, Denk W, Kerr JN. Two-photon calcium imaging of evoked activity from L5 somatosensory neurons in vivo. *Nat Neurosci.* 2011; 14(8):1089–1093. [PubMed: 21743473]
- Murari, K., Etienne-Cummings, R., Cauwenberghs, G., Thakor, N. An integrated imaging microscope for untethered cortical imaging in freely-moving animals. *Engineering in medicine and biology society (EMBC); 2010 annual international conference of the IEEE; IEEE.* 2010.
- Murari, K., Greenwald, E., Etienne-Cummings, R., Cauwenberghs, G., Thakor, N. Design and characterization of a miniaturized epiilluminated microscope. *Engineering in medicine and biology society, 2009; EMBC 2009. Annual international conference of the IEEE; IEEE.* 2009.
- Murari K, Li N, Rege A, Jia X, All A, Thakor N. Contrast-enhanced imaging of cerebral vasculature with laser speckle. *Applied Optics.* 2007; 46(22):5340–5346. [PubMed: 17676149]
- Murayama M, Perez-Garci E, Luscher HR, Larkum ME. Fiberoptic system for recording dendritic calcium signals in layer 5 neocortical pyramidal cells in freely moving rats. *J Neurophysiol.* 2007; 98(3):1791–1805. [PubMed: 17634346]
- Murayama M, Pérez-Garci E, Nevian T, Bock T, Senn W, Larkum ME. Dendritic encoding of sensory stimuli controlled by deep cortical interneurons. *Nature.* 2009; 457(7233):1137–1141. [PubMed: 19151696]
- Mutoh H, Perron A, Akemann W, Iwamoto Y, Knöpfel T. Optogenetic monitoring of membrane potentials. *Experimental physiology.* 2011; 96(1):13–18. [PubMed: 20851856]
- Nasrallah I, Dubroff J. An overview of PET neuroimaging. *Semin Nucl Med.* 2013; 43(6):449–461. [PubMed: 24094712]
- Ng DC, Tamura H, Mizuno T, Tokuda T, Nunoshita M, Ishikawa Y, Shiosaka S, Ohta J. An implantable and fully integrated complementary metal-oxide semiconductor device for in vivo neural imaging and electrical interfacing with the mouse hippocampus. *Sensors and Actuators a-Physical.* 2008; 145:176–186.
- Ng DC, Tokuda T, Shiosaka S, Tano Y, Ohta J. Implantable microimagers. *Sensors.* 2008; 8(5):3183–3204. [PubMed: 27879873]
- O’Sullivan TD, Heitz RT, Parashurama N, Barkin DB, Wooley BA, Gambhir SS, Harris JS, Levi O. Real-time, continuous, fluorescence sensing in a freely-moving subject with an implanted hybrid VCSEL/CMOS biosensor. *Biomed Opt Express.* 2013; 4(8):1332–1341. [PubMed: 24009996]
- Osman, A., Park, JH., Dickensheets, D., Platasa, J., Culurciello, E., Pieribone, VA. A head-mountable microscope for high-speed fluorescence brain imaging. *Biomedical Circuits and Systems Conference (BioCAS), 2011 IEEE; IEEE.* 2011.

- Osman A, Park JH, Dickensheets D, Platasa J, Culurciello E, Pieribone VA. Design Constraints for Mobile, High-Speed Fluorescence Brain Imaging in Awake Animals. *Biomedical Circuits and Systems*, IEEE Transactions on. 2012
- Park JH, Platasa J, Verhagen JV, Gautam SH, Osman A, Kim D, Pieribone VA, Culurciello E. Head-mountable high speed camera for optical neural recording. *J Neurosci Methods*. 2011; 201(2):290–295. [PubMed: 21763348]
- Petersen CC, Grinvald A, Sakmann B. Spatiotemporal dynamics of sensory responses in layer 2/3 of rat barrel cortex measured in vivo by voltage-sensitive dye imaging combined with whole-cell voltage recordings and neuron reconstructions. *The Journal of Neuroscience*. 2003; 23(4):1298–1309. [PubMed: 12598618]
- Piyawattanametha W, Cocker ED, Burns LD, Barretto RPJ, Jung JC, Ra H, Solgaard O, Schnitzer MJ. In vivo brain imaging using a portable 2.9 g two-photon microscope based on a microelectromechanical systems scanning mirror. *Optics Letters*. 2009; 34(15):2309–2311. [PubMed: 19649080]
- Rege A, Thakor NV, Rhie K, Pathak AP. In vivo laser speckle imaging reveals microvascular remodeling and hemodynamic changes during wound healing angiogenesis. *Angiogenesis*. 2012; 15(1):87–98. [PubMed: 22198198]
- Saunter C, Semprini S, Buckley C, Mullins J, Girkin J. Micro-endoscope for in vivo widefield high spatial resolution fluorescent imaging. *Biomedical optics express*. 2012; 3(6):1274–1278. [PubMed: 22741074]
- Sawinski J, Wallace DJ, Greenberg DS, Grossmann S, Denk W, Kerr JN. Visually evoked activity in cortical cells imaged in freely moving animals. *Proc Natl Acad Sci U S A*. 2009; 106(46):19557–19562. [PubMed: 19889973]
- Senarathna, J., Murari, K., Etienne-Cummings, R., Thakor, N. Design of a novel head-mountable microscope system for laser speckle imaging. *Biomedical Circuits and Systems Conference (BioCAS)*, 2011 IEEE; IEEE. 2011.
- Senarathna J, Murari K, Etienne-Cummings R, Thakor NV. A Miniaturized Platform for Laser Speckle Contrast Imaging. *Ieee Transactions on Biomedical Circuits and Systems*. 2012; 6(5):437–445. [PubMed: 23853230]
- Senarathna J, Rege A, Li Thakor N. Laser Speckle Contrast Imaging: Theory, Instrumentation and Applications. *IEEE Reviews in Biomedical Engineering*. 2013
- Szuts TA, Fadeyev V, Kachiguine S, Sher A, Grivich MV, Agrochao M, Hottowy P, Dabrowski W, Lubenov EV, Siapas AG, Uchida N, Litke AM, Meister M. A wireless multi-channel neural amplifier for freely moving animals. *Nat Neurosci*. 2011; 14(2):263–269. [PubMed: 21240274]
- Theer P, Hasan MT, Denk W. Two-photon imaging to a depth of 1000  $\mu\text{m}$  in living brains by use of a Ti:  $\text{Al}_2\text{O}_3$  regenerative amplifier. *Optics Letters*. 2003; 28(12):1022–1024. [PubMed: 12836766]
- Theuwissen AJP. CMOS image sensors: State-of-the-art. *Solid-State Electronics*. 2008; 52(9):1401–1406.
- Ts'o DY, Frostig RD, Lieke EE, Grinvald A. Functional organization of primate visual cortex revealed by high resolution optical imaging. *Science*. 1990; 249(4967):417–420. [PubMed: 2165630]
- Tye KM, Deisseroth K. Optogenetic investigation of neural circuits underlying brain disease in animal models. *Nat Rev Neurosci*. 2012; 13(4):251–266. [PubMed: 22430017]
- Zhang J, Campbell RE, Ting AY, Tsien RY. Creating new fluorescent probes for cell biology. *Nat Rev Mol Cell Biol*. 2002; 3(12):906–918. [PubMed: 12461557]

### Highlights

- Advances in optics and microelectronics have made miniaturized imagers feasible.
- *In vivo* neuroimaging in unrestrained/unanesthetized animals is now a reality.
- Miniaturized imagers have provided new insights on brain organization and function.
- We highlight the advances in fabrication and applications of miniaturized imagers.
- We discuss strengths and weaknesses, and future potential of miniaturized imagers.

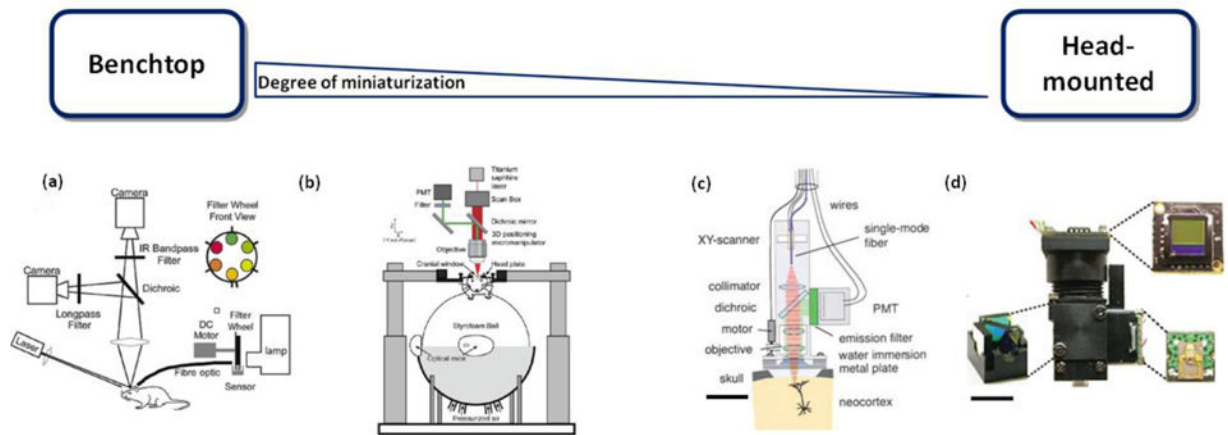


### Figure 1. Evolution of benchtop to 'head-mounted' neuroimaging systems

The degree of miniaturization increases from (a)–(d). (a) A dual modality benchtop system for simultaneous multispectral imaging and laser speckle contrast imaging in anesthetized animals (Jones et al. 2008). (b) Schematic of the system setup for imaging in head-restrained, awake mice (Dombeck et al. 2007). The head-mounted imaging system was modified from a standard two-photon microscope. The head of each mouse was restrained while the animal moved on a treadmill for behavioral testing. (c) Additionally miniaturized fiber-optics-based system (Helmchen et al. 2001), in which the photomultiplier tube (PMT) was incorporated into the head piece, wherein the excitation light was still derived from a benchtop system. The head piece was 7.5 cm long (Scale bar = 23.5 mm). (d) An integrated head-mounted system (Ghosh et al. 2011), using surface mounted LEDs for excitation and a miniaturized CMOS sensor for detection (Scale bar = 5 mm). This self-contained system enabled experiments involving interactive and natural animal behaviors. All images have been adapted with permission of the publishers.

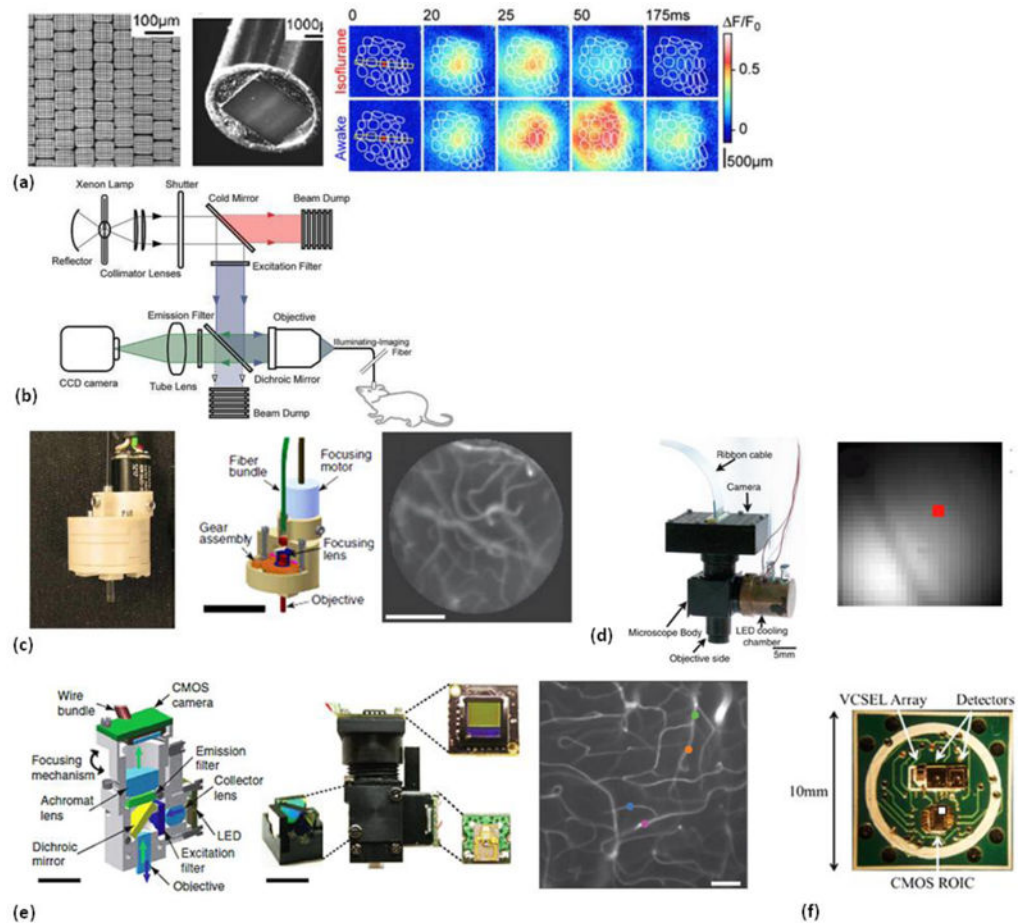


### Figure 2. Miniaturized single-photon optical systems

(a) Images of the custom manufactured fiber optic bundle from (Ferezou et al. 2006), based on wound image bundle technology (Schott Fiber Optics, Southbridge MA). The left panel shows a high-magnification image of the fiber bundle tips: each group consisted of 6 fibers; each fiber had 8 μm cores and a resulting numerical aperture of 0.6. The middle panel shows an image of the fiber bundle (diameter ~ 5 mm) that was in direct contact with rat cortex. The right panel shows a comparison of the cortical responses to C2 whisker deflections imaged by voltage-sensitive dye (VSD) using the fiber optic image bundle in a mouse while it was either under isoflurane anesthesia or awake. (b) Single-fiber system schematic for side-on imaging of pyramidal cells in layer 5 of the rat neocortex (Murayama et al. 2007). The fiber bundle was used to transmit excitation light and collect fluorescence signals from a standard benchtop system. (c) Fiber optic single-photon microscope from (Flusberg et al. 2008), showing the head mount comprising of focusing optics, the fiber bundle and focusing motor. The head piece weighed 1.1 g, and the system had a frame rate of less than 100 Hz. The two GRIN objective lenses of different focal lengths enabled deep (6.2mm) and superficial tissue (1.4mm) imaging. The right panel shows an image of the neocortical vasculature from an awake, freely moving mouse (Scale bar = 100 μm). (d) A self-contained fluorescence microscope (Osman et al. 2012), consisting of a LED light source, CMOS image sensor, focusing optics and excitation/emission filters. The microscope was designed for high-speed imaging and detecting small changes ( $< 1\% \Delta F/F$ )

in fluorescence signals. The right panel shows an image of the barrel cortex labeled with VSD. The image was captured using the sensor in (Osman et al. 2012) and a tandem inverted lens microscope. (e) Self-contained one-photon microscope (Ghosh et al. 2011), light source (LED) and image sensor (CMOS camera) were mounted on the head piece (weight ~ 1.9g). The electrical signal was transmitted via the wire bundle to a FPGA, for both LED control and image acquisition. The microvasculature of a freely behaving mouse was acquired after injection of fluorescein-dextran. The image is the standard deviation computed from a ten second acquisition, to emphasize the vasculature. (Scale bar = 50  $\mu\text{m}$ ) (f) Photograph of the VCSEL-CMOS sensor reported by (O'Sullivan et al. 2013). The custom PCB with bonded chips, consists of multiple VCSEL excitation sources, two GaAs photodiodes and a CMOS read-out integrated circuit (ROIC). All images have been adapted with permission of the publishers.

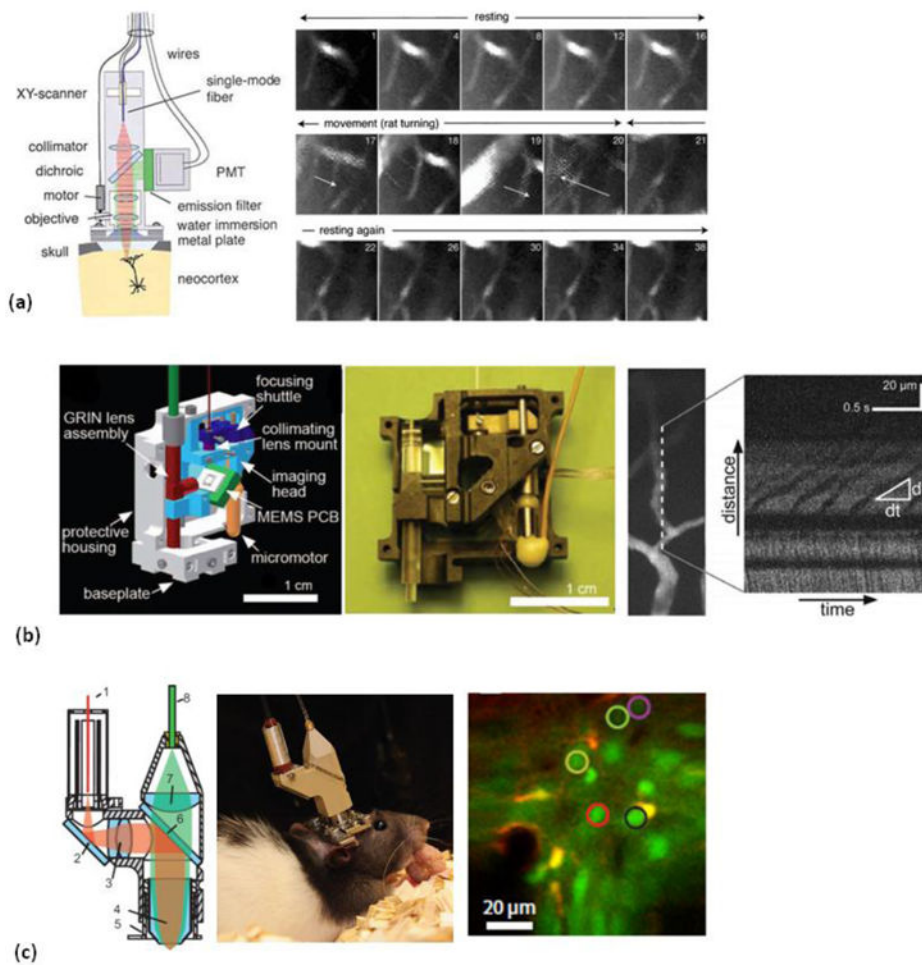


### Figure 3. Miniaturized two-photon optical systems

(a) Left panel: The first reported head-mounted two-photon microscope (Helmchen et al. 2001). Near infrared laser excitation was coupled to a single mode fiber, collimated and focused by a water-immersion objective to the neocortex. Fluorescence signal collection was achieved by a PMT. Right panel: Sample images from an awake rat labeled with fluorescein-dextran (0.5 s frame duration). Motion caused the FOV to shift from frame 17 to 20 (indicated by white arrows). (b) Schematic (left) and photograph (middle) of the two-photon microscope based on a MEMS scanning mirror (Piyawattanametha et al. 2009). The microscope weighed 2.9 g, excitation pulse and fluorescence collection were separated by using two different types of optic fibers, which enhanced the SNR of the detected fluorescence signals. Right panel: Images of neocortical capillaries from an anesthetized adult mouse injected with fluorescein isothiocyanate-dextran dye. Line scanning mode (shown in the enlarged view on the right) allowed the microscope to track individual erythrocytes flowing parallel to the line scanning direction. (c) Left panel: Schematic of the two-photon microscope, made up of: 1. single-mode excitation fiber; 2. folding mirror; 3. tube lens; 4. objective; 5. focusing flange; 6. beam splitter; 7. collimation lens; 8. multi-mode collection fiber. Middle panel: Photograph of a rat with the head-mounted microscope (Sawinski et al. 2009); Right panel: Overlay of *in vivo* images acquired using two

fluorescent dyes: SRS 101 that labels astrocytes (red channel) and the calcium indicator OGB-1 that labels neurons (green channel), in a rat's visual cortex. The colored circles indicate the neurons and the astrocyte (red circle) from which signals were analyzed in response to visual stimulation.

Author Manuscript

Author Manuscript

Author Manuscript

Author Manuscript

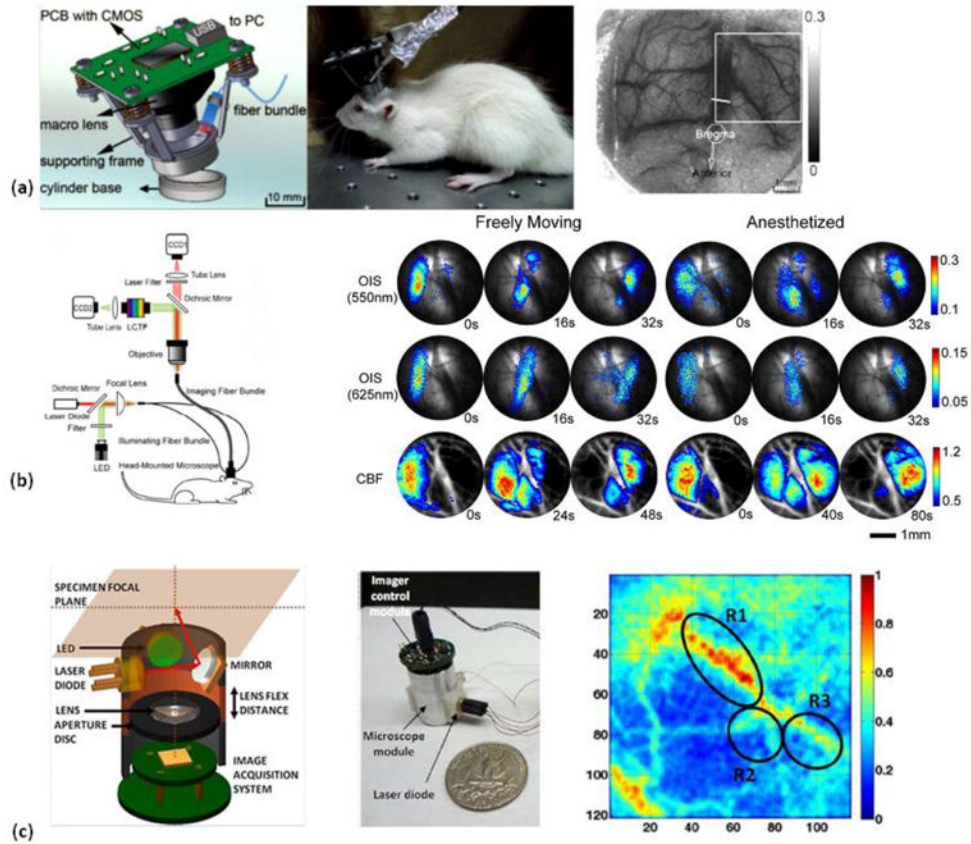


**Figure 4. Miniaturized optical systems that utilize endogenous contrast agents**

(a) Left panel: Schematic of a fiber-optics-based laser speckle imaging microscope. The illumination was fiber-coupled from a benchtop laser source and the camera chip was incorporated within the head piece. Middle panel: A rat with the head-mounted microscope that was ~ 20 g in weight and 3.1 cm in height. Right panel: *In vivo* laser speckle contrast image from a freely moving rat after co-registration (Miao et al. 2011). The image shows the vascular network in the rat cortex over a 7 mm × 7 mm FOV. (b) Left panel: Schematic of dual-modal fiber-optic-based microscope designed by (Liu et al. 2013). The system consisted of three parts: a fiber-coupled dual illumination source, a head-mounted microscope and two CCD cameras system for dual modality acquisition. Right panel: Spatio-temporal evolution of hemodynamic changes from a cortical spreading depression (CSD) model illustrating the difference between anesthetized and awake states (Liu et al. 2013). (c) Schematic (left panel) and photograph (middle panel) of a self-contained laser speckle imaging microscope in which light from a VCSEL is reflected by a side mirror to accommodate different focal planes. The speckle signals were focused onto a custom made CMOS sensor by a single lens (Senarathna et al. 2012). Right panel: Relative blood flow map derived from speckle contrast images acquired using the microscope in (f) (laser wavelength  $\lambda = 795$  nm) from the rat cortex over a ~1.85 mm × 2 mm FOV. The higher blood flow velocity of R1 indicates that R2 and R3 are downstream of R1 and that blood flow from R1 is branching off into R2 and R3.

Table 1

Summary of miniaturized and mobile brain imaging systems.

Single-photon exogenous contrast microscopes:						
Contrast Agent	Weight	Size	Field of View	In-plane Resolution	Temporal Resolution	Application Reference
VSD (RHI 691)	N/A	N/A	3 × 3 mm <sup>2</sup>	N/A	2 ms per frame	Whisker barrel cortex imaging (Ferezou et al. 2006)
Fluorescein-dextran, Ca <sup>2+</sup> indicator (Oregon green)	1.1 g	N/A	0.07 mm <sup>2</sup>	~ 2.8–3.9 μm	Up to 100Hz	Blood flow speed/distribution, Ca <sup>2+</sup> dynamics of Purkinje cells (Flusberg et al. 2008)
GCaMP3	N/A	N/A	4 mm <sup>2</sup>	N/A	N/A	Ca <sup>2+</sup> imaging of Glia cells (Cha et al. 2014)
VSD (RHI 692)	10 g	N/A	4.88 mm <sup>2</sup>	25 μm	Up to 900 Hz	Whisker barrel cortex imaging (Osman et al. 2012)
Fluorescein-dextran, Ca <sup>2+</sup> indicator (Oregon green)	1.9 g	N/A	~ 0.5 mm <sup>2</sup>	~ 2.5 μm	36Hz or 100Hz	Blood flow speed/distribution, Ca <sup>2+</sup> dynamics of Purkinje cells (Ghosh et al. 2011)
Cy 5.5 dye	0.7 g	1 cm <sup>3</sup>	N/A	N/A	N/A	N/A (O'Sullivan et al. 2013)
Two-photon exogenous contrast microscopes:						
Contrast Agent	Weight	Size	Field of View	Lateral Resolution	Temporal Resolution	Application Reference
Fluorescein-dextran Ca <sup>2+</sup> indicator (green-1)	25 g	7.5 cm long	N/A	Dendritic spines resolved	N/A	N/A (Helmchen et al. 2001)
Fluorescein-dextran Rhodamine	N/A	N/A	0.8 mm diameter	Lateral: 2.5 μm Axial: 20 μm	N/A	N/A (Göbel et al. 2004)
Fluorescein-dextran	2.9 g	2×1.9×1.1 cm <sup>3</sup>	N/A	Lateral: 1.29±0.05 μm Axial: 10.3±0.3 μm	1-15Hz	Blood flow analysis (Piyawattanametha et al. 2009)
GAD67-GFP	~ 1.5 g	N/A	300 μm diameter	Lateral: 3.2±0.4 μm Axial: 5.1±1 μm	N/A	N/A (Engelbrecht et al. 2010)
Sulforhodamine 101 & Ca <sup>2+</sup> indicator	5.5 g	N/A	N/A	Single soma resolved	90 ms per frame	Ca <sup>2+</sup> dynamics from visual stimuli (Sawinski et al. 2009)
Calcium indicator	0.6 g	N/A	Up to 200 μm	Lateral: 0.98±0.09 μm Axial: 7.68±1.3 μm	25 Hz	Ca <sup>2+</sup> dynamics of Purkinje cells (Engelbrecht et al. 2008)
Endogenous contrast microscopes:						
Contrast Agent	Weight	Size	Field of View	Lateral Resolution	Temporal Resolution	Application Reference
LSCI	~ 20 g	3.1 cm long	N/A	16 lp/mm	N/A	Vasculature/relative blood flow (Miao et al. 2011)
LSCI & Multispectral	1.5 g	N/A	N/A	5.5 μm	N/A	Cortical spreading depression (Liu et al. 2013)
LSCI	~ 7 g	5 cm <sup>3</sup>	3.5×3.3 mm	N/A	6 Hz	Vasculature/relative blood flow (Senarathna et al. 2012)

N/A = Microscope specifications were 'not available' in the referenced publication.